

Charging Network Design and Service Pricing for Electric Vehicles With User-Equilibrium Decisions

Amir Mirheli^{ID} and Leila Hajibabai^{ID}, *Member, IEEE*

Abstract—This paper aims to investigate the electric vehicle (EV) charging network design and utilization management considering user-centric decisions. A hierarchical formulation is developed with the EV charging network design and demand-driven pricing scheme in the upper level and users' charging decisions to minimize their own travel costs and charging expenses in the lower level. The model aims to minimize the facility deployment cost and maximize the charging income of the network operator while minimizing the user-centric costs. We have converted the proposed bi-level formulation into an equivalent single-level model using the lower-level objective function as complementary equations. Then, we have developed an iterative active-set based solution technique to determine the strategic decisions on charging network design. To partially overcome the computational burden, the arc travel times are estimated using a macroscopic fundamental diagram concept. The proposed integrated methodology is applied to a hypothetical and an empirical case study to evaluate its performance and solution quality. The numerical results indicate that the proposed algorithm can solve the problem efficiently and outperform a system-level bi-level optimization benchmark. Our experiments show a CPU time of 2.3 *hr* for the proposed approach compared to 173.1 *hr* of the benchmark. Finally, a series of sensitivity analyses has been conducted to study the impact of input parameters on the solutions and draw managerial insights.

Index Terms—Bi-level, active-set, pricing, hierarchical, electric vehicle, network design.

I. INTRODUCTION

ELECTRIC mobility services promise significant sustainability benefits by reducing environmental pollution caused by the transportation sector. While EVs and accompanied automation breakthroughs are predicted to trigger a significant transformation of transportation systems, the market share of EVs and plug-in hybrids remains small, i.e., 2.1% in 2019 [1]. Large-scale adoption of electric mobility is hampered by a variety of factors among which, inadequate public charging infrastructure and the absence of user-responsive charging services (e.g., access to desired charging slots and locations considering travel and charging expenses) play a major role. In other words, EV's limited on-board battery capacity, inappropriate location of charging facilities, limited adaptability of market prices to the underlying demand, and

Manuscript received 13 September 2021; revised 15 May 2022, 23 July 2022, and 3 October 2022; accepted 28 November 2022. Date of publication 31 January 2023; date of current version 1 March 2023. The Associate Editor for this article was B. Singh. (*Corresponding author: Leila Hajibabai.*)

Amir Mirheli is with the Operations Research Program, Department of Industrial and Systems Engineering, North Carolina State University, Raleigh, NC 27695 USA (e-mail: amirhel@ncsu.edu).

Leila Hajibabai is with the Department of Industrial and Systems Engineering, North Carolina State University, Raleigh, NC 27695 USA (e-mail: lhajiba@ncsu.edu).

Digital Object Identifier 10.1109/TITS.2022.3227888

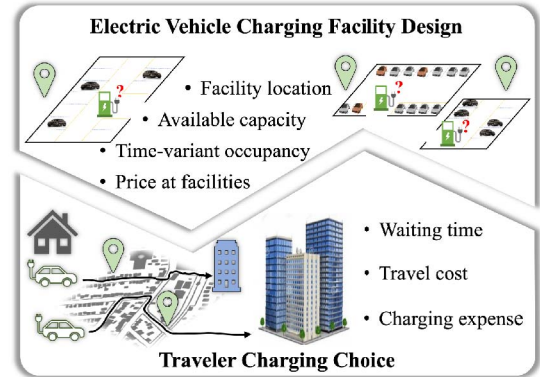


Fig. 1. Interactions of EV charging facility utilization and travel flow.

long wait times on top of the already lengthy charging times discourage customers from wide usage of the existing technology, especially for long trips or trip chains. The diversity of EV users' preferences (e.g., toward charger location, charging price, waiting time to get served) exacerbates the challenge. While fast chargers can provide enough energy within an hour of charging time for several short trips, their infrastructure can be very costly, e.g., \$50K or more per charger [2]. This affects the physical capacity (i.e., number of chargers) of fast charging facilities. Thus, there is a need to locate charging facilities with optimal capacities and dynamically allocate resources to users with time-variant prices and minimal wait times over the usage periods, while maximizing the utilization of facilities. The dynamic pricing scheme will facilitate the utilization of charging facilities given demand variations over time. For instance, a high price at a low-demand location does not help with attracting customers, while an extremely low price at a high-demand area may not be profitable to the agency either. This motivates a demand-driven pricing scheme based on the perspectives of both agency (e.g., profitability) and customers (e.g., charger availability and cost). Figure 1 presents the inter-relationship between EV charging facility design and EV users' charging choices. The optimal plan shall satisfy the charging demand and regulate the utilization of charging facilities to accommodate both users' and charging network operators' objectives and help expand the market share of EVs.

This paper explores EV charging network design and utilization management accounting for user-centric decisions. Currently, EV charging prices are set by the charging operator and are not necessarily coordinated across various locations in a region or a city nor over time (i.e., prices can change temporally but often not via an algorithm). A dynamic demand-driven pricing scheme can support the utilization of

charging facilities given the perspectives of charging operators and users. A hierarchical formulation is developed with the charging network design and demand-driven pricing scheme in the upper level and EV users' charging decisions in the lower level. The model aims to minimize facility deployment and operating costs as well as user-centric costs. The proposed framework will determine solutions for charging facility locations along with dynamic charging prices and resource allocations to users. Note that power distribution network constraints are not included in this study. It is assumed that the power grid can provide the required electricity to charging locations. The proposed methodology is applied to hypothetical and real-world case studies to evaluate its performance and draw managerial insights. The numerical experiments confirm the solution quality of the proposed algorithm in comparison to an exact benchmark approach.

The exposition of the paper is as follows. The next section reviews the literature in the context of EV charging and route planning. Section III presents a mathematical formulation for the joint optimization of network design and time-variant pricing of charging facilities with equilibrium decisions. Section IV explains the proposed approach to solve the problem and Section V illustrates the numerical results. Finally, Section VI summarizes the findings and discusses future research directions.

II. LITERATURE REVIEW

Existing literature on the EV charging present EV operations under pre-defined versus unknown charging locations. While the first category considers EV travel and charging decisions solely with existing charging facilities, the latter aims to further facilitate the charging logistics by incorporating the charging network design (i.e., location and capacity) into EV route optimization models. The relevant literature to this study cover (i) charging location and route planning models and (ii) user-centric and equilibrium models.

A. Charging Location and Route Design Models

Literature presents research efforts on deterministic EV charging location models such as Ghamami et al. [3] that have used a fixed-charge facility location model to find the optimal location and capacity of plug-in electric vehicle (PEV) charging lots. Additionally, Zheng and Peeta [4] have introduced an auxiliary network based on the EV travel range limitation, with arc lengths less than a defined threshold. The problem aims to find the optimal charger locations that minimize the total facility installation costs considering fixed demand and station capacity. A Benders decomposition is applied to find the solution with a small optimality gap. Later, Li et al. [5] have implemented the government strategy to promote the EV use by minimal infrastructure development using a bi-level model structure. The upper level captures the government's infrastructure decisions, while the lower level aims to minimize the operating cost of EV companies through their optimal fleet composition and route plan. A hybrid heuristic approach is used to solve the problem that includes (i) a variable neighborhood descent to select charging facility locations and (ii) a scatter search to determine

the route plan. The traffic conditions are not incorporated into the routing decisions and the system-level optimality of scatter search is not verified. Besides, a series of studies has focused on flow-capturing location models that aim to install a fixed number of charging facilities to maximize the flows on paths with charging stations [6], [7], [8], [9]. Berman and Larson [10] have introduced a charging facility location problem for PHEVs as a generalization of the flow re-fueling location problem. Their arc-cover model aims to maximize vehicles-miles-traveled (VMT) using electricity considering both EV and PHEVs. A benders decomposition is used to solve the problem that is improved by Pareto-optimal cut generation schemes. Lee and Han [11] have also extended the flow re-fueling location model using a probability function that captures the impact of various factors such as road conditions on travel range. The model is solved by a combined Bender-and-Price method that integrates benders decomposition and column generation techniques. This study does not account for the impact of traffic congestion on network travel times.

Literature also presents studies that capture the impact of stochasticities (e.g., random demand or stochastic user behavior) on network design models. For instance, Li et al. [12] have formulated the EV sharing locations with corresponding EV fleet size into a stochastic model under the dynamic demand and non-linear vehicle charging duration. A continuum approximation approach is used that splits the problem into smaller neighborhoods and approximates each by an infinite homogeneous plane. In addition, Faridimehr et al. [13] have developed a two-stage stochastic model, where the first stage determines the location and number of charging stations and the second stage assigns the EVs to their preferred charging lots (based on their willingness to walk) to maximize the expected access to public charging facilities. The model includes uncertainties in EV demand flows, charging patterns, arrival and departure times, travel purposes, and preferred walking distances. A sample average approximation method is used to generate a large number of scenarios (i.e., location and capacity of charging stations) in the two-stage stochastic program. Large-scale cases are solved using heuristics, where their solution quality is not verified. Later, Xie et al. [2] have proposed a multi-stage chance-constrained model to find the location and number of chargers considering the actual trip demand. The model aims to minimize total cost including the (i) fixed and variable charging facility installation and (ii) penalty cost if BEV trips are not completed due to the range limitation. A genetic algorithm is applied to solve the problem, where the system-level optimality is not guaranteed. Furthermore, Hua et al. [14] have developed an integrated charging network design and fleet operation policy for one-way EV sharing services. A multi-stage stochastic model is proposed to address the time-varying uncertain demand using a Monte Carlo sampling technique. A tree search algorithm is used to solve certain scenarios based on demand levels to facilitates finding solutions.

B. User-Centric and Equilibrium Models

A school of research also accounts for user-centric factors and equilibrium decisions [15], [16], [17], [18]. For instance,

[19] have developed a bi-level model structure with charging facility deployment in the upper level and user-equilibrium (UE) traffic assignment subject to travel range limitation in the lower level. Feasibility of all paths are checked based on the sufficiency of battery level to complete all travels using range auxiliary variables. This study defines the cost function based only on the length of traversing paths, where user-centric factors (e.g., charging price) are overlooked. Additionally, He et al. [20] have developed a strategic planning model to determine the optimal plug-in hybrid electric vehicle (PHEV) charging facility locations. The study shows that PHEV interactions, for travel time and charging cost minimization, results in an equilibrium condition on traffic flow, charging price, and power flow distribution. An active-set algorithm is employed to solve the problem. The strategic charging facility design does not fully satisfy the time-variant demand, particularly in high-demand neighborhoods. Moreover, [21] have developed a bi-level program that aims to minimize the total travel time and charging facility deployment cost with a UE assignment for a mixed EV and internal combustion engine vehicle traffic. The proposed model is solved using the cross-entropy method that randomly samples the location of charging facilities and update them iteratively to push the solutions toward optimality. The study does not account for the EV users' perspectives on charging price, waiting time, or so forth. Similarly, [22] have formulated a multi-type recharge facility location problem as a bi-level program. The upper level aims to minimize the total travel cost under limited roadway capacity expansion budget and provisions of EV charging facilities. The lower level represents the UE traffic assignment for internal combustion engine vehicles and EVs. This study has applied a genetic algorithm procedure to find the solution for roadway capacity expansion decisions and recharge facility sites. He et al. [23] have also proposed a bi-level tour-based formulation to optimize the charging network design. The network equilibrium model also accounts for BEV users' risk-taking attributes given their SOC and limited driving range. To calculate the required energy on each path, the traversing distance is used independent of traffic flow. An iterative approach based on genetic algorithm is used to tackle the model complexity due to tour enumerations. Furthermore, He et al. [24] have developed a bi-level program to determine the optimal charging network design considering the driving range limitation and required charging duration by a path-based equilibrium traffic assignment. Rather than the amount of flow captured by charging facilities, the objective function models the maximum flow that can use charging facilities en-route. The proposed model does not consider multiple charging attempts in long-distance trips. Furthermore, [25] have explored the competitiveness of charging lanes for charging in motion by analyzing equilibrium choice of charging facilities given (i) number and capacity of charging stations, (ii) length of charging lanes, and (iii) charging prices at both types of facilities in a long traffic corridor. The study aims to minimize social costs versus agency profits. On the other hand, [26] have identified the location of wireless charging facilities and incorporated stochastic UE in a FCLM. Besides, [27] have formulated a bi-level model to maximize the demand coverage of BEVs

in the upper level and analyze a stochastic UE in the lower level.

C. Summary

Studies on electrified mobility investigate strategic or operational factors concerning range-constrained travel behaviors, charging network design, charging network operator perspectives, or electric vehicle user preferences. The existing models either (1) assume a fixed charging price in each time interval regardless of the location of chargers; (2) define the cost function based only on the length of traversing paths, ignoring user-centric factors (e.g., price, wait time); (3) account for operator perspectives and user behaviors independently without seeking an equilibrium solution; (5) assume chargers are always available; (6) consider travel times as fixed and independent of traffic impacts on routing decisions; or (7) frequently apply solution techniques that do not sufficiently balance the computational efficiency and solution quality (e.g., meta-heuristics) when dealing with complex multi-level models.

While the existing literature also presents models that incorporate emission considerations [28], extreme fast charging technologies [29], battery swap studies [30], charge scheduling [31] in car-sharing systems [32], intercity travels [33], among other innovative solutions (e.g., see [34], [35], [36], [37]), our paper specifically focuses on the charging location and pricing design given a set of user-centric factors. The main contribution of this paper is developing an integrated framework for the facility location design and dynamic pricing of EV chargers under UE decisions. A stochastic queuing theory is utilized to establish a linear relationship between each facility's occupancy and physical capacity. The problem is formulated as a bi-level optimization program, where network design and management decisions are modeled in the upper level and user response (with respect to charging prices, locations, and wait times to get served at the facilities) are captured in the lower level. The objective is to minimize (i) facility deployment and charging costs and (ii) user costs including travel and charging expenses. The bi-level formulation is converted into an equivalent single-level program, following the redefinition of binary location decision variables as continuous variables, by transforming the lower-level objective function to complementary equations. The problem is then solved using an active-set methodology that determines the EV charging facility allocation plan. Additionally, to partially reduce the computational complexity of finding UE flows, a macroscopic fundamental diagram (MFD) concept, incorporated into the method of successive average (MSA), is implemented to estimate the arc travel times, instead of using highly non-linear arc performance functions. Finally, to evaluate the quality of the solutions, a benchmark solution technique is implemented that generates theoretical bounds to the proposed bi-level problem.

III. MODEL FORMULATION

This section introduces a bi-level model, where the upper level aims to minimize the costs associated with charging network design and maximize the revenue obtained from chargers. The lower level aims to minimize the user-centric costs on travel

TABLE I
DEFINITION OF SETS, VARIABLES, AND PARAMETERS

Sets	
Γ	Set of all time steps, i.e., $\{0, 1, \dots, T-1\}$
N	Set of nodes
A	Set of arcs
A_i^-, A_i^+	Set of inbound and outbound arcs to and from node $i \in N$
OD	Set of origin-destination
λ_{od}^t	Set of users with $od \in OD$ at time $t \in \Gamma$
\mathcal{R}	Set of regions in an urban network
\mathcal{M}^{od}	Set of paths among od 's
Var.	
y_i	Binary; 1 if there is a facility at $i \in N$, or 0 O.W.
η_i	Number of chargers at node $i \in N$
p_i^t	Price of getting charge at node $i \in N$ at time $t \in \Gamma$
σ_{od}^t	Equilibrium disutility identical for users on $od \in OD$ at time t
$x_a^{t,od,i}$	Flow of arc $a \in A$ from $od \in OD$ to charge at $i \in N$ at time t
$z_a^{t,od}$	Flow of arc $a \in A$ from $od \in OD$ at time t
v_a^t	Arc flow at arc $a \in A$ at time t
$R_a^t(v_a^t)$	Travel time of arc $a \in A$ at time t
$c_a^{t,od}$	Binary; 1 if $a \in A$ is on a feasible path for EVs on $od \in OD$ at time t , or 0 O.W.
u_i^{od}	Maximal distance traveled from the last visited facility at node $i \in N$ with $od \in OD$
$u_i'^{od}$	Dummy variable, 0 at facility located at $i \in N$
ϕ	Function of each facility's physical capacity η_i and occupancy f_i^t at time t
ζ	Probability function of waiting duration at each facility i to find a vacant charger
$\rho_i^{t,od}$	Minimal cost to get to node $i \in N$ from origin $o \in O$ to destination $d \in D$ at time t
v_r^t	Number of accumulated users in region $r \in \mathcal{R}$ at time t
$\Upsilon_r(v_r^t)$	Production rate in region $r \in \mathcal{R}$ at time t
Π_r^t	Trip completion rate in region $r \in \mathcal{R}$ at time t
$l_{r,m}^{t,od}$	Total trip length on path m across region r
Par.	
α	Positive coefficient representing the operation period (e.g., # of days per year)
b	Elasticity coefficient of the demand function
B	Available budget for charging facility deployment
C_i	Unit cost of installing charging facility at node $i \in N$
χ^δ	Step size at iteration δ in the MSA algorithm
η_{max}	Maximal physical capacity of each charging facility
f_i^t	Occupancy of facility at node $i \in N$ at time t
g_{od}^t	Intercept of the linear demand curve for EV travellers on $od \in OD$ at time t
κ	Lower bound for probability of finding a vacant charger
l_i	Lower bound for charging price at node $i \in N$
\mathcal{L}	Driving range limit of EVs
M	Large positive constant
μ_a	Length of arc $a \in A$
ν	Cruising time window for finding a vacant charger
Ω_i	Slope of the linear waiting function at node $i \in N$
θ	Average charging duration
l_i'	Upper bound for charging price at node $i \in N$
ξ_i^t	EV arrival rate in node $i \in N$ at time t
V_r^t	Average speed in region $r \in \mathcal{R}$ at time t

and charging expenses. Table I presents the notations used in the model formulation.

We introduce the spatial and temporal elements of the problem, as follows. Let T denote the number of discrete time periods in the planning horizon and $\Gamma = \{0, 1, \dots, T-1\}$ represent the set of all time periods at which charging decisions are made. The transportation network is defined by $G(N, A)$, with N as the set of nodes (including the candidate

nodes for charging facilities) and A as the set of arcs. Here, $A_i^- \subset A$ and $A_i^+ \subset A$ define the set of inbound and outbound network arcs to and from node $i \in N$, respectively.

We define decision variable $y_i \in \{0, 1\}$ to represent the charging facility deployment decisions at node $i \in N$. Accordingly, decision variable $\eta_i \in \mathbb{Z}$ denotes the physical capacity (i.e., number of EV chargers) of a facility installed at node i . The decision variable p_i^t determines the charging price of facility i at each time t . We let state variable f_i^t capture the occupancy of each charging facility at node $i \in N$ over time $t \in \Gamma$. Besides, we let $x_a^{t,od,i}$ represent the EV flow, visiting charging facility at node $i \in N$ at time $t \in \Gamma$, on arc $a = (i, j) \in A$ from $o \in O$ to $d \in D$, where O and D denote the sets of origins and destinations, respectively. To capture the UE traffic flow, a non-negative variable $z_a^{t,od}$ is defined to represent the flow of arc a on $od \in OD$ at time t . Besides, v_a^t denotes the aggregated flow on arc a at time t . The user-centric demand λ_{od}^t follows a $H(\sigma_{od}^t)$ form that is an inverse demand function of the equilibrium disutility σ_{od}^t for demand on $od \in OD$ at time t . Thus, $|\lambda_{od}^t| = H(\sigma_{od}^t)$ represents the set of users who travel from $o \in O$ to $d \in D$ at time t [38], [39].

Finding a vacant charger at each node i within ν cruising time can be presented by an Erlang C formula in queuing theory as a stochastic chance logic, similar to [2]. We define ϕ to represent the waiting time at charging facility i as a function of facility's occupancy f_i^t and physical capacity η_i . Function $\phi(f_i^t, \eta_i)$ helps find the waiting time based on EVs' arrival rate and their expected service time. The Erlang C formula expresses the probability ζ of being served in a pre-defined time-window by forming a queue of EV users; i.e., $\zeta(\phi(f_i^t, \eta_i) \leq \nu)_i^t$, where ν represents the cruising time-window. We define a targeted service level by

$$\zeta(\phi(f_i^t, \eta_i) \leq \nu)_i^t \geq \kappa, \quad \forall i \in N, t \in \Gamma, \quad (1)$$

which defines a lower bound κ for the probability of finding a vacant charger at i within ν cruising time. Each facility (with η_i chargers) serves a queue with an expected service time θ and EV arrival rate ξ_i^t at time t . Hence, the left-hand side of (1) can be expanded as

$$\begin{aligned} \zeta(\phi(f_i^t, \eta_i) \leq \nu)_i^t &= 1 - \frac{(\xi_i^t \theta)^{\eta_i}}{\eta_i!} \left(\frac{(\xi_i^t \theta)^{\eta_i}}{\eta_i!} \right. \\ &\quad \left. + \left(1 - \frac{\xi_i^t \theta}{\eta_i}\right) \sum_{q=0}^{\eta_i-1} \frac{(\xi_i^t \theta)^q}{q!} \right)^{-1} \\ &\quad \times e^{-(\eta_i - \xi_i^t \theta) \nu \theta^{-1}}, \\ &\quad \forall i \in N, t \in \Gamma, \end{aligned} \quad (2)$$

which establishes a non-linear relationship among η_i , ξ_i^t , θ , and ν . Equation (2) can be illustrated as a step function using the available information on θ and the targeted service level. The feasible region of charging facility capacities (e.g., $0 \leq \eta_i \leq \eta_{max}$) will be divided into equal sub-regions, and a new set of binary variables will be defined for the maximum occupancy of charging facility on each sub-region. For instance, Figure 2, hypothetically, shows the relationship between each facility's maximum occupancy and physical

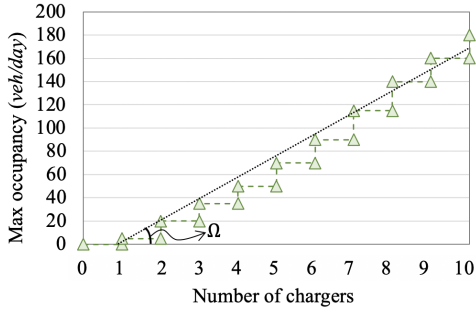


Fig. 2. Relationship of maximal occupancy and number of chargers.

capacity with 95% probability to find a vacant charger within 10 min.

The step function presented in Figure 2 can be defined as piece-wise linear functions. However, it introduces additional binary variables to the problem that makes it more challenging. Without loss of generality, we utilize a linear function to capture the impact of waiting time on maximal occupancy assuming that waiting time can be reduced if there is always a vacant charging spot. Thus, Figure 2 introduces a new upper bound for maximal occupancy based on the capacity of each facility, as

$$f_i^t \leq \Omega_i \eta_i, \quad \forall i \in N, t \in \Gamma, \quad (3)$$

where Ω_i represents the slope of the linear approximation function that provides an upper bound on facility i 's occupancy. Note that the newly defined upper bound is less than η_i by defining $\Omega_i \leq 1, \forall i \in N$, which limits the number of served users to restore the vacant charging spot at all time steps.

The integrated charging facility design and management scheme is modeled into a bi-level mathematical optimization program, where charging facility manager's perspective is formulated in the upper level, as follows.

$$\min_{y, \eta, p} \sum_{i \in N} (\eta_i C_i - \alpha \sum_{t \in \Gamma} \sum_{a \in A} \sum_{od \in OD} p_i^t x_a^{t, od, i}), \quad (4a)$$

$$\text{subject to } l_i y_i \leq p_i^t \leq l'_i y_i, \quad \forall i \in N, t \in \Gamma, \quad (4b)$$

$$f_i^t = f_i^{t-1} - \sum_{od \in OD} \sum_{a \in A_i^+} x_a^{t, od, i} + \sum_{od \in OD} \sum_{a \in A_i^-} x_a^{t, od, i} \quad \forall i \in N, t \in \Gamma \setminus \{0\}, \quad (4c)$$

$$\sum_{od \in OD} \sum_{a \in A_i^-} x_a^{t, od, i} \leq \eta_i - f_i^{t-1}, \quad \forall i \in N, t \in \Gamma \setminus \{0\}, \quad (4d)$$

$$f_i^t \leq \eta_i, \quad \forall i \in N, t \in \Gamma, \quad (4e)$$

$$\lambda_{od}^t = H(\sigma_{od}^t) = g_{od}^t - b \sigma_{od}^t, \quad \forall od \in OD, t \in \Gamma, \quad (4f)$$

$$\sum_{i \in N} \eta_i C_i \leq B, \quad (4g)$$

$$\eta_i \leq M y_i, \quad \forall i \in N, \quad (4h)$$

$$\eta_i \leq \eta_{max}, \quad \forall i \in N, \quad (4i)$$

$$y_i \in \{0, 1\}, \quad \forall i \in N. \quad (4j)$$

The upper-level objective function (4a) simultaneously (i) minimizes the EV charging facility installation cost and (ii) maximizes the revenue gained by charging payment collections. Parameter C_i represents the unit installation cost for a single EV charger deployed at node $i \in N$. And, α is a positive coefficient representing the operation period of a facility (e.g., the number of operating days annually). Constraints (4b) define a lower bound l_i and upper bound l'_i for charging price p_i^t at time t , if a charging facility is available at node i , i.e., $y_i = 1$. Constraints (4c) represent the flow conservation, i.e., state transition functions on facility occupation. Constraints (4d) show that demand flow should not exceed the available capacity at node i , calculated by excluding the existing occupancy prior to time t from physical capacity at node i . Constraints (4e) ensure that the occupancy of each facility at node i at time t is less than the facility's physical capacity. Constraints (4f) represent the inverse demand function, obtained from [40], that capture the impact of charging prices on the charging demand. The equilibrium disutility σ_{od}^t represents the minimum cost imposed to EV users due to (1) charging price p_i^t at charging facility $i \in N$ and time t and (2) travel time from origin $o \in O$ to charging facility i and beyond (i.e., final destination $d \in D$). Note that σ_{od}^t is identical for all EV users on the same $od \in OD$ at time t . The term g_{od}^t is the intercept of the demand curve for EV travellers with $od \in OD$ at time t . Additionally, budget constraints on EV charger deployments are shown by (4g). Constraints (4h) ensure that EV chargers can only be available at node i if there is an open facility at i . We let M be a large positive constant. Constraints (4i) define a limit η_{max} for physical capacity of each charging facility. Finally, constraints (4j) shows the charging facility deployment decisions are binary variables.

The lower-level problem represents the EV user reactions to total costs (i.e., travel time and charging expenses) that affect their facility selection. Travel time on arc $a \in A$ follows an increasing function of aggregated EV flow v_a^t , i.e., $R_a^t(v_a^t)$. We define non-negative auxiliary variables u_i^{od} and $u_i'^{od}$ at each node $i \in N$ to represent the driving range constraints. Variable u_i^{od} denotes the maximum distance traveled from the last visited charging facility at node i on a path with $od \in OD$. Additionally, $u_i'^{od}$ is a dummy variable that is zero at facilities. The feasible travel paths are defined based on the EV driving range. Binary variable $c_a^{t, od}$ identifies the arcs located on feasible paths, where $c_a^{t, od} = 1$ if arc a is on a feasible path containing $od \in OD$ at time t , or 0 otherwise. To address the EV driving range limitation and ensure that the users travel on feasible paths, i.e., within their maximum driving range unless there is (at least) a charging facility en-route, we use the following equations (also see [19]). EVs are assumed to start their travels with an ample initial SOC to reach charging facilities and that they leave the facilities with sufficient SOC to arrive at their final destinations.

$$z_a^{t, od} \leq M c_a^{t, od}, \quad \forall a \in A, od \in OD, t \in \Gamma, \quad (5a)$$

$$u_j^{od} \geq u_i^{od} + \mu_a - M(1 - c_a^{t, od}), \quad \forall a = (i, j) \in A, od \in OD, t \in \Gamma, \quad (5b)$$

$$u_i^{od} \leq \mathcal{L}, \quad \forall i \in N, od \in OD, \quad (5c)$$

$$u_i^{od} \geq u_i^{od} - M y_i, \forall i \in N, od \in OD, \quad (5d)$$

$$u_i^{od} \leq u_i^{od} + M y_i, \forall i \in N, od \in OD, \quad (5e)$$

$$u_i^{od} \leq M(1 - y_i), \forall i \in N, od \in OD, \quad (5f)$$

$$u_i^{od} \geq 0, u_i^{od} \geq 0, \forall i \in N, od \in OD, \quad (5g)$$

where $\mu_a > 0$ represents the length of arc $a \in A$ and \mathcal{L} denotes the driving range limit. Constraints (5a) enforce EV flow to choose arcs that are located on the feasible path. Constraints (5b) ensure the auxiliary variable u_j^{od} is updated for all $j \in N$ and $od \in OD$ based on the distance μ_a traveled on the feasible path. Then, constraints (5c) ensure that EVs will not violate their driving range. Constraints (5d)-(5e) confirm that $u_i^{od} = u_i^{od}$ if there is no facility at node i . Constraints (5f) impose $u_i^{od} = 0$ when there is a facility at node i ; here, M represents a large positive value. And, constraints (5g) indicate the non-negativity of u_i^{od} and u_i^{od} . Finally, user behaviors on the choice of charging facilities are captured by

$$\min_{v,x,z} \sum_{t \in \Gamma} \sum_{a \in A} \left(\int_0^{v_a^t} R_a^t(\omega) d\omega + \gamma \sum_{i \in N} \sum_{od \in OD} p_i^t x_a^{t,od,i} \right) \quad (6a)$$

subject to (5a) – (5g) and

$$v_a^t = \sum_{od \in OD} z_a^{t,od}, \quad \forall a \in A, t \in \Gamma, \quad (6b)$$

$$x_a^{t,od,i} \leq z_a^{t,od}, \quad \forall a = (i, j) \in A, \quad (6c)$$

$$\begin{aligned} od \in OD, t \in \Gamma, \\ \sum_{a \in A_i^+} z_a^{t,od} - \sum_{a \in A_i^-} z_a^{t,od} = \\ \begin{cases} \lambda_{od}^t, & \forall i \in O \\ -\lambda_{od}^t, & \forall i \in D \\ 0, & \text{o.w.} \end{cases} \quad \forall od \in OD, t \in \Gamma, \end{aligned} \quad (6d)$$

$$x_a^{t,od,i} \geq 0, z_a^{t,od} \geq 0, \quad \forall a = (i, j) \in A, \quad (6e)$$

$$v_a^t \geq 0, \quad \forall a \in A, t \in \Gamma. \quad (6f)$$

The lower-level problem aims to minimize the individual users' costs, including their travel time and charging expense following an equilibrium condition. It shows that users choose shortest routes that include charging facilities en-route. Function $R_a^t(\omega)$ captures the impact of traffic flows on arc travel times. Parameter γ is the cost-to-monetary value conversion factor. Constraints (5a)-(5g) represent EV driving range limit to ensure users drive on paths that are within their maximum range given their SOC. Constraints (6b) define the aggregated arc flows at each time t . Constraints (6b)-(6f) represent an equilibrium traffic assignment for EV users on sub-networks with feasible paths, where destinations are within EVs' maximum driving range unless there is at least a charging facility en-route, for each origin-destination pair. Therefore, the lower-level problem represents the routing and charging behavior of EV users by tracking their SOC. In particular, constraints (6c) show the flow feasibility; they ensure that the charging demand at node i , i.e., the start node

of arc $a = (i, j)$, does not exceed the flow passing through arc a at time t . Note that flow $x_a^{t,od,i}$ indicates the portion of EV users who get charged at $i \in N$, which unilaterally affects objective function (4a) and (6a) until no improvement can be achieved. Constraints (6d) illustrate the conservation of user flows at each node i ; i.e., $\sum_{a \in A_i^+} z_a^{t,od} = \sum_{a \in A_i^-} z_a^{t,od}$ unless i is either the origin or destination of user demand. Finally, constraints (6e) and (6f) show the non-negativity of travel flows.

Let us further explain how the lower-level problem functions: Given the charging network design (i.e., the location and capacity of charging facilities), the lower-level problem (5a)-(5g) and (6a)-(6f) is formulated as an integrated distribution and assignment model [41]. The charging facilities are assumed as destinations with the utility of p_i^t , where EV users aim to access charging facilities that yield minimum travel time, cruising time, and charging expenses. If we let u_{oi}^t denote the travel time of the minimum EV path from origin $o \in O$ to charging facility at node $i \in N$ at time $t \in \Gamma$, EV users will try to access charging facilities that yield the minimum net travel impedance $u_{oi}^t + p_i^t$. Note that based on the Wardrop's first principle [41], EV users cannot unilaterally improve the net travel impedance by switching to other paths and/or charging facilities. This condition represents a UE distribution and assignment model, where the objective of each user is optimized individually. UE decisions facilitate more accurate modelling of (i) user responses to charging prices, travel time to charging facilities, waiting time to get served, charger availability, among other factors, (ii) user responses to other users' decisions, and (iii) charging network operator's responses to users' decisions.

IV. SOLUTION TECHNIQUE

The proposed formulation (4a)-(4i), (5a)-(5g), and (6a)-(6f) has a bi-level form and contains mixed-integer decision variables and non-linear terms. To tackle the complexities, an integrated solution technique is developed that includes (i) an active-set algorithm and (ii) an MFD based strategy. The details are illustrated in Sections IV-A and IV-B, respectively.

A. Active-Set Technique

The proposed mixed-integer non-linear program (MINLP) is computationally intractable given the integer physical capacity η , due to additional branching at each integer solution. Hence, it is beneficial to redefine the integer variables as follows. We first define the physical capacity η_i of charging facility at i as a combination of new binary location variables y'_{ik} ; i.e.,

$$\eta_i = \sum_{k=0}^K 2^k y'_{ik}, \quad \forall i \in N, \quad (7a)$$

$$y'_{ik} \in \{0, 1\}, \quad \forall i \in N, k \in K, \quad (7b)$$

where $K = \lceil \log_2 \eta_{max} \rceil$ and η_{max} indicates the maximal number of chargers. Therefore, constraints (4i) can be relaxed given a pre-determined upper bound for K . Furthermore, y'_{ik}

can relax the binary network design decision variable y_i to a continuous variable in $[0, 1]$:

$$y_i \geq y'_{ik}, \quad \forall i \in N, k \in K, \quad (8a)$$

$$y_i \leq \sum_{k=0}^K y'_{ik}, \quad \forall i \in N. \quad (8b)$$

Literature has shown the relaxation of binary decision variables $y'_{ik} \in \{0, 1\}$, $\forall i \in N, k \in K$ to continuous variables $0 \leq y'_{ik} \leq 1$, using complementary constraints $y'_{ik}(1 - y'_{ik}) = 0$. An active-set based technique relaxes the need for the complementary constraints and tackles the associated complexities, as also shown in [42] and [20]; otherwise, the binary decisions do not allow the derivation of dual slackness to satisfy the complementary slackness conditions [43].

We now reformulate the proposed bi-level MINLP (3), (4a)-(4i), (5a)-(5g), (6a)-(6f), (7a)-(7b), and (8a)-(8b) as an equivalent single-level program using Karush-Kuhn-Tucker (KKT) conditions, similar to [44]. We introduce $\rho_i^{t,od}$ as a minimum cost to get to node $i \in N$ from origin $o \in O$ to destination $d \in D$ at time t . Hence, the lower-level objective function (6a) will be transformed into complementary equations, similar to [45], as

$$\begin{aligned} 0 &\leq R_a^t(v_a^t) \\ &+ \gamma p_i^t x_a^{t,od,i} - \rho_i^{t,od} + \rho_j^{t,od} \perp z_a^{t,od} \geq 0, \\ &\forall a = (i, j) \in A, \quad od \in OD, \quad t \in \Gamma. \end{aligned} \quad (9)$$

Note that all the aforementioned terms are defined over $[0, \infty)$ domain and they form a cone in \mathbb{R}^2 and \mathbb{R} . Therefore, the solution to the complementary equations will be the same as those to the variational inequalities [46]. We can re-write (9) as linear equations, using (5a), as illustrated below.

$$\begin{aligned} 0 &\leq R_a^t(v_a^t) \\ &+ \gamma p_i^t x_a^{t,od,i} - \rho_i^{t,od} + \rho_j^{t,od} \leq M(1 - c_a^{t,od}), \\ &\forall a \in A, \quad od \in OD, \quad t \in \Gamma. \end{aligned} \quad (10)$$

We add variable $\rho_i^{t,od}$ to the upper-level objective function (4a) to capture the total cost of individual users. The bilinear term $\mathbf{p} \mathbf{x}$ in (10) is converted into a set of tangent supporting planes using a piece-wise linear function. The equivalent single-level MINLP formulation is

$$\begin{aligned} \mathcal{A} : \quad &\min_{y, \eta, y', \mathbf{p}, \mathbf{v}, \mathbf{z}, \mathbf{x}, \rho} \sum_{i \in N} (\eta_i C_i - \\ &\alpha \sum_{i \in \Gamma} \sum_{a \in A} \sum_{od \in OD} \rho_i^{t,od}) \\ &\text{subject to (4b) - (4g), (5a) - (5g), (6b) - (6f),} \\ &\text{(7a) - (7b), (8a) - (8b), and (10).} \end{aligned} \quad (11)$$

Note that the impact of charging price p_i^t is captured in the calculation of $\rho_i^{t,od}$ in constraints (10); hence, objective function (11) does not include a separate term to account for the network operator's revenue.

The approach generates the charging facility network design (i.e., location and physical capacity) and modifies it iteratively. Given the charging network plan, the problem can be converted

into integrated distribution and assignment models [41], solvable using commercial solvers, e.g., CPLEX [47]. The information on charging facility locations and network geometry identifies the arcs located on feasible paths. Thus, $c_a^{t,od}$ will be relaxed to a continuous variable (i.e., $0 \leq c_a^{t,od} \leq 1$) to satisfy the duality theory.

We define active sets Δ_1 , Δ_0 , and Δ , where Δ_1 contains selected network nodes to install charging facilities, Δ_0 includes nodes with no charging facility, and $\Delta = \{(i, k) : i \in N, k = 0, \dots, K\}$. Note that $\Delta_0 \cap \Delta_1 = \emptyset$ and $\Delta_0 \cup \Delta_1 = \Delta$. We re-formulate \mathcal{A} based on the active sets as

$$\min_{y, \eta, y', \mathbf{p}, \mathbf{v}, \mathbf{z}, \mathbf{x}, \rho} \sum_{i \in N} (\eta_i C_i - \alpha \sum_{i \in \Gamma} \sum_{a \in A} \sum_{od \in OD} \rho_i^{t,od}) \quad (12a)$$

subject to (4b) - (4g), (5a) - (5g), (6b) - (6f),

(7a), (8a) - (8b), (10), and

$$y'_{ik} = 0, \quad \forall (i, k) \in \Delta_0, \quad (12b)$$

$$y'_{ik} = 1, \quad \forall (i, k) \in \Delta_1. \quad (12c)$$

At iteration n , the allocation plan of network nodes to Δ_1^n and Δ_0^n will be updated to ensure optimal charging locations will be found over a finite number of iterations; also see [42]. The active-set procedure follows.

Step 0 Initialize the active sets: set $n = 1$, $\Delta_0^1 = \Delta$, and $\Delta_1^1 = \emptyset$ (i.e., assume no charging facility is installed on nodes $i \in N$).

Step 1 Determine the solution to decision variables $\eta, y, y', \mathbf{p}, \mathbf{f}, \mathbf{x}, \mathbf{v}, \mathbf{z}$, and ρ using (Δ_0^n, Δ_1^n) . Find ω_{ik}^n and μ_{ik}^n , the smallest and largest values of KKT multipliers associated with constraints (12b)-(12c). Set E^n as the total cost (12a) associated with the current allocation plan.

Step 2 Set $Q = -\infty$ and adjust the active sets:

Step 2.1 Solve the following knapsack problem to determine \mathbf{w}^* and \mathbf{b}^* .

$$\min_{w, b} \sum_{(i,k) \in \Delta_0^n} \omega_{ik}^n w_{ik} - \sum_{(i,k) \in \Delta_1^n} \mu_{ik}^n b_{ik} \quad (13a)$$

$$\begin{aligned} \text{subject to} \quad &\sum_{(i,k) \in \Delta_0^n} C_i 2^k w_{ik} - \\ &\sum_{(i,k) \in \Delta_1^n} C_i 2^k b_{ik} \leq B - \sum_{(i,k) \in \Delta_1^n} C_i 2^k \end{aligned} \quad (13b)$$

$$\begin{aligned} &\sum_{(i,k) \in \Delta_0^n} \omega_{ik}^n w_{ik} - \\ &\sum_{(i,k) \in \Delta_1^n} \mu_{ik}^n b_{ik} \geq Q, \end{aligned} \quad (13c)$$

$$w_{ik}, b_{ik} \in \{0, 1\}. \quad (13d)$$

Obtaining $w_{ik} = 1$ from the knapsack formulation implies that node i shall be moved from Δ_0^n to Δ_1^n to modify the node allocation plan; otherwise, $b_{ik} = 1$ leads to shifting (i, k) from Δ_1^n to Δ_0^n (i.e., no need to deploy charging facility at i). Terminate the algorithm if the optimal objective value (13a) is zero (i.e., the allocation plan cannot

be further improved) and set the current solution as optimal. Otherwise, go to *Step 2.2* to update the plan \mathbf{y}'' based on (Δ'_0, Δ'_1) .

Step 2.2 Set

$$U = \sum_{(i,k) \in \Delta_0^n} \omega_{ik}^n w_{ik}^* - \sum_{(i,k) \in \Delta_1^n} \mu_{ik}^n b_{ik}^*, \quad (14a)$$

$$\begin{aligned} \Delta'_0 &= (\Delta_0^n - [(i,k) \in \Delta_0^n : w_{ik}^* = 1]) \\ &\cup [(i,k) \in \Delta_1^n : b_{ik}^* = 1], \end{aligned} \quad (14b)$$

$$\begin{aligned} \Delta'_1 &= (\Delta_1^n - [(i,k) \in \Delta_1^n : b_{ik}^* = 1]) \\ &\cup [(i,k) \in \Delta_0^n : w_{ik}^* = 1]. \end{aligned} \quad (14c)$$

Step 2.3 Evaluate the quality of the updated plan: solve problem (12a)-(12c) using (Δ'_0, Δ'_1) and compare the objective value (12a) to E^n . Go to *Step 2.4* if total infrastructure and operating cost (12a) using (Δ'_0, Δ'_1) is less than E^n . Otherwise, set $Q = U + \epsilon$, where $\epsilon > 0$, and return to *Step 2.1*.

Step 2.4 Set $\Delta_0^{n+1} = \Delta'_0$, $\Delta_1^{n+1} = \Delta'_1$, and $n = n + 1$. Go to *Step 1*.

Proposition 1 ensures that an optimal solution to (12a)-(12c) exists for a feasible allocation plan. Additionally, Theorem 1 shows that a proper adjustment in the allocation plan will reduce the charging facility deployment cost and increase the revenue.

Proposition 1: Given binary vector $\bar{\mathbf{y}}$, compatible with complete and budget-feasible active pairs (Δ_0^n, Δ_1^n) at iteration n , we have: $\bar{y}'_{ik} = 0, \forall (i,k) \in \Delta_0^n$, and $\bar{y}'_{ik} = 1, \forall (i,k) \in \Delta_1^n$. We let $(\bar{\mathbf{z}}, \bar{\mathbf{v}})$ be the solution to the UE problem: $0 \leq R_a^t(v_a^t) + \gamma p_i^t x_a^{t,od,i} - \rho_i^{t,od} + \rho_j^{t,od} \perp z_a^{t,od} \geq 0, \forall a \in A$. Then, $(\bar{\mathbf{y}}', \bar{\mathbf{z}}, \bar{\mathbf{v}})$ is the optimal solution to (12a)-(12c).

Proof: Given a monotone travel time function $R_a^t(v_a^t)$, the solution $(\bar{\mathbf{z}}, \bar{\mathbf{v}})$ to the UE problem is unique. Thus, $(\bar{\mathbf{y}}', \bar{\mathbf{z}}, \bar{\mathbf{v}})$ must be the optimal solution as it is the only feasible solution to equilibrium problem: $0 \leq R_a^t(v_a^t) + \gamma p_i^t x_a^{t,od,i} - \rho_i^{t,od} + \rho_j^{t,od} \perp z_a^{t,od} \geq 0$. \square

Furthermore, pairs (Δ_0^n, Δ_1^n) at iteration n are complete partitions and every feasible solution to problem (12a)-(12c) is feasible to original problem \mathcal{A} .

Theorem 1: If $\omega_{i'k'} < 0$ for some $(i', k') \in \Delta_0^n$ and $\mu_{i'k'} > 0$ for some $(i', k') \in \Delta_1^n$ at iteration n , then the solution to \mathcal{A} will be improved by adjusting $\Delta_0^n = \Delta_0^n - (i', k')$ and $\Delta_1^n = \Delta_1^n + (i', k')$, respectively.

Proof: The adjustments to active sets Δ_0^n and Δ_1^n at iteration n suggest relaxing the binding constraints for some (i', k') in the minimization problem (12a)-(12c), which may provide a lower objective value. A non-decreasing trend in the objective value adjustments (i.e., no solution improvements) suggests that constraints $y'_{ik} \geq 0$ and $y'_{ik} \leq 1$ are binding, which contradicts with the properties of their associated multipliers: $\omega_{i'k'} < 0$ and $\mu_{i'k'} > 0$. For more details; see Theorem 1 and 2 in [42]. \square

Theorem 1 indicates that the adjustment plan in *Step 2.1* will suggest the optimal modification of active sets (Δ_0^n, Δ_1^n) ,

which will minimize the costs imposed to the charging network operator.

B. Travel Time Estimation

This section introduces an MFD-based method to estimate travel times imposed to EVs traveling on each arc. Note that while most studies in the literature (e.g., [48]) capture the impact of traffic flows on arc travel times using the performance function developed by Bureau of Public Roads [49], the fourth-degree polynomial form of the monotonic BPR function imposes additional computational complexities to the problem. MFD, with a more aggregated nature, estimates the travel times by constructing a relationship between traffic flow, density, and speed in the transportation network [50], which is still applicable to regions (e.g., arcs) of an urban network with homogeneous distribution of traffic congestion [51]. Figure 3, hypothetically, presents (i) an urban network divided into different homogeneous regions $r \in \mathcal{R}$ and (ii) several paths $m \in \mathcal{M}^{od}$ that connect origin $o \in O$ to destination $d \in D$. The region boundaries are defined based on the network geometry and traffic distribution. A unique trip production rate $\Upsilon_r(v_r^{t'})$ corresponding to the accumulated number of users $v_r^{t'}$ in region r at time t is defined, which shows total VMT by EV users in each region in unit time. The accumulated number of users on path $m \in \mathcal{M}^{od}$ in region r at time t is denoted by $v_{r,m}^{t,od}$ that can be updated based on flow $z_a^{t,od}$, as follows.

$$\begin{aligned} v_{r,m}^{t,od} &= z_{a|a \in A_r^+ \cap a \in m}^{t,od} - z_{a|a \in A_r^- \cap a \in m}^{t,od} \\ &\quad + \mathbf{1}_o(r) \lambda_{od,m}^{t,od}, \quad \forall r \in \mathcal{R}, m \in \mathcal{M}^{od}, \\ &\quad od \in OD, t \in \Gamma, \end{aligned} \quad (15)$$

where A_r^+ and A_r^- represent the inbound and outbound arcs to region r , respectively. In this equation, $\mathbf{1}_o(r)$ is 1 if the origin is located in region r , or 0 otherwise. We let $\lambda_{od,m}^{t,od}$ denote the share of user-centric demand $\lambda_{od}^{t,od}$ who choose path m . Equation (15) defines the accumulated number of users $v_{r,m}^{t,od}$ by (i) the generated demand on path $m \in \mathcal{M}^{od}$ with $od \in OD$ if region r is origin o at time t , (ii) the inbound flows from upstream arcs on path m , and (iii) the outbound flows to downstream arcs.

Let Π_r^t denote the trip completion rate that represents the number of EV users who leave region r at time t . We represent total trip length on path m across region r by $l_{r,m}^{t,od}$. Similarly, $\Pi_{r,m}^{t,od}$ denotes the trip completion rate in region r for users traveling on path m with $od \in OD$ at time t , as follows [50]:

$$\begin{aligned} \Pi_{r,m}^{t,od} &= \frac{\Upsilon_r(v_r^{t'})}{v_r^{t'}} \frac{v_{r,m}^{t,od}}{l_{r,m}^{t,od}} = V_r^t \frac{v_{r,m}^{t,od}}{l_{r,m}^{t,od}}, \quad \forall r \in \mathcal{R}, \\ &\quad m \in \mathcal{M}^{od}, \quad od \in OD, t \in \Gamma, \end{aligned} \quad (16)$$

where V_r^t denotes the average speed in region r . Trip completion rate $\Pi_{r,m}^{t,od}$ represents the number of users on path $m \in \mathcal{M}^{od}$ who complete their trip within region $r \in \mathcal{R}$ at time t . Note that (16) establishes a relationship between speed V_r^t and density $\frac{v_{r,m}^{t,od}}{l_{r,m}^{t,od}}$ to compute trip production rate $\Pi_{r,m}^{t,od}$ in region r at time t . Hence, travel time on each arc $a \in \mathcal{R}$ can



Fig. 3. A multi-region urban network.

be estimated by

$$R_a^t(v_a^t) = v_a^t \left(\sum_{od \in OD} \sum_{m \in \mathcal{M}^{od}} \Pi_{r,m}^{t,od} \right)^{-1}, \quad \forall a \in \mathcal{R}, t \in \Gamma. \quad (17)$$

According to (16), trip completion rate is obtained by the (i) accumulated number of users $v_r^{t,t}$ and (ii) average trip length in each region r at time t . The accumulated number of users $v_r^{t,t}$ in each region r can be obtained from (15) by incorporating the solution to \mathcal{A} (using the active-set technique in IV-A). Note that total trip length $l_{r,m}^{t,od}$ on path m across region r indirectly represents the traffic condition on path m in region r . We implement an iterative algorithm to estimate the total trip length in each region r over iteration δ , keeping the same trip completion rate (to reach a traffic equilibrium) on each od at time t . We first set the total trip length $l_{r,m}^{t,od,1}$ to the length of arcs on path m in region r . Then, we solve (12a)-(12c) using the proposed active-set method to find the traffic flow on each arc. We then find the accumulated number of users $v_r^{t,t}$ and trip completion rate $\Pi_{r,m}^{t,od}$ using (15) and (16), respectively. Afterwards, the average trip lengths will be adjusted as follows.

$$l_{r,m}^{t,od,\delta+1} = l_{r,m}^{t,od,\delta} + (\delta + 1)^{-1} (l_{r,m}^{t,od} - l_{r,m}^{t,od,\delta}), \quad \forall r \in \mathcal{R}, m \in \mathcal{M}^{od}, od \in OD, t \in \Gamma, \quad (18)$$

where $l_{r,m}^{t,od}$ represents the adjustment of total trip length for users with $od \in OD$ on path m . Note that (18) applies the difference between total trip lengths in the update procedure using $l_{r,m}^{t,od}$ and the predetermined step size (i.e., $\frac{1}{\delta+1}$) at iteration δ . To achieve traffic equilibrium, the average trip completion rates $\bar{\Pi}_{r,m}^{t,od}$ are calculated as follows.

$$\bar{\Pi}_{r,m}^{t,od} = \frac{\sum_{m \in \mathcal{M}^{od}} \Pi_{r,m}^{t,od}}{|\mathcal{M}^{od}|}, \quad \forall r \in \mathcal{R}, m \in \mathcal{M}^{od}, od \in OD, t \in \Gamma, \quad (19)$$

where the variance of each path from the average trip completion rate is obtained as $\Pi_{r,m}^{t,od} - \bar{\Pi}_{r,m}^{t,od}$. Then, the adjustment of total trip length $l_{r,m}^{t,od}$ is formulated as an inverse function of the variances at iteration δ (i.e., $l_{r,m}^{t,od} = V_r^t v_{r,m}^{t,od} (\Pi_{r,m}^{t,od} - \bar{\Pi}_{r,m}^{t,od})^{-1}$). The problem (12a)-(12c) is solved again until the difference of trip production rate in two consecutive iterations is within a pre-defined threshold ε' . Figure 4 presents the proposed algorithm to find the charging facility location along with the UE traffic assignment.

The aforementioned iterative MFD-based algorithm utilizes the MSA method, where the arcs' travel times R_a^t are updated

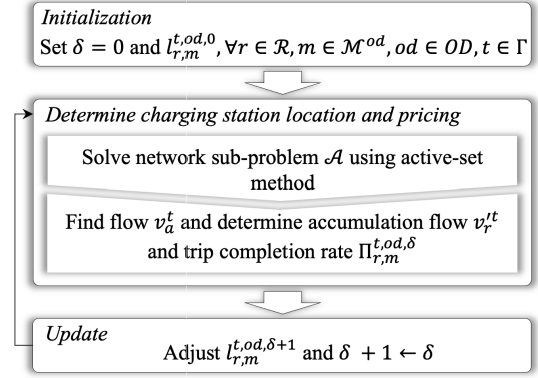


Fig. 4. Flowchart of the proposed algorithm.

at each iteration δ until the algorithm converges. We introduce $l_m^{*t,od} = \min\{l_{r,m}^{*t,od}, \forall r \in \mathcal{R}\}$ as the optimal total trip length for EV users with $od \in OD$ on path $m \in \mathcal{M}^{od}$. The main objective of the MSA method is to find $l_m^{*t,od}$ via an iterative procedure using the step size $\chi^\delta = (\delta + 1)^{-1}$, as indicated in (18). [52] have shown the convergence proof of MSA [53].

V. NUMERICAL EXPERIMENTS

The solution technique proposed in Section IV is coded in Java and run on a desktop computer with quad-core 3.6 GHz CPU and 16 GB of memory. A Poisson distribution is applied to generate the initial demand pattern for five different time-of-days in a business day, i.e., early AM, AM peak, mid-day, PM peak, and evening. Commercial solver LINDO [54] is utilized to solve model (12a)-(12c) and find the multipliers associated with constraints (12b)-(12c).

A. Hypothetical Dataset

To verify the applicability of the proposed methodology, we first apply our model (4b)-(4g), (5a)-(5g), (6b)-(6f), (7a)-(7b), (8a)-(8b), (10), and (11) and hybrid solution framework to a hypothetical network. The planning horizon is assumed to be from 8 AM to 5:30 PM with the time interval of 30 min. The network dataset includes 12 nodes and 32 arcs. We assume EV users need one time period (e.g., 30 min) to get charged. The average vehicle arrivals over different time-of-days is respectively assumed to be 20, 25, 20, 15, and 30 for early AM, AM peak, mid-day, PM peak, and evening for a medium demand level. Accordingly, the low and high demand levels are assumed to be half and twice the medium demand, respectively. The available budget is assumed to be \$500K and the deployment cost of each charger is \$50K. An arc elasticity coefficient for the demand function is assumed to be $b = -0.3$ to capture the impact of disutility on charging demand.

The value of objective function parameter α is set to 365 that represents the number of days in a year assuming the same demand distribution in different days. Note that a series of sensitivity analysis has been conducted to show the impact of α on the objective value (see Section V-C). Besides, the maximum driving range is set to 200 miles to study the impact of driving range limitation on the solutions. We also set the

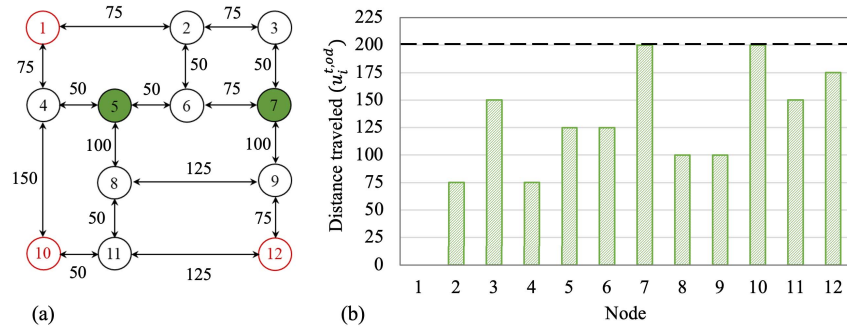


Fig. 5. (a) Selected charging facilities (demand from node 1 to nodes 10 & 12); (b) Max distance traveled from the last visited charging facility.

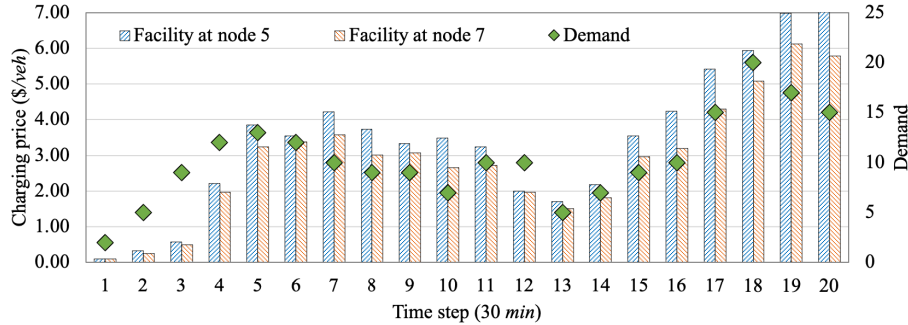


Fig. 6. Charging price at facilities 5 and 7 over the planning horizon.

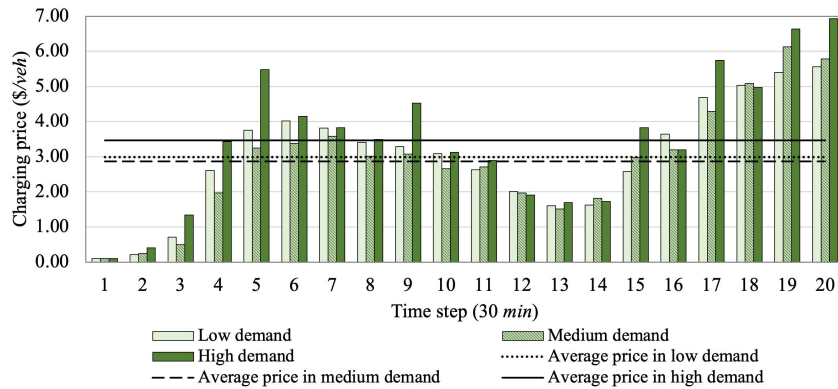


Fig. 7. Average charging price at candidate facilities over the planning horizon.

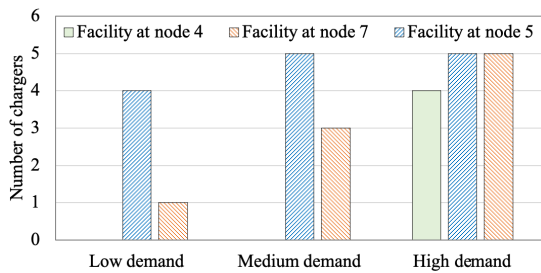


Fig. 8. Number of selected chargers in different demand levels.

slope value Ω_i of the linear waiting function as $\Omega_i = 0.85$ for candidate facility $i \in N$. Finally, we assume that a maximum of five chargers can be installed at each selected facility. We also assume $l'_i = 10.0(\$/veh)$ and $l_i = 0.1(\$/veh)$, $\forall i \in N$, which respectively represent the maximum and minimum charging prices at chargers per time step.

1) *Results:* Figure 5(a) shows the selected locations of charging facilities originated from node 1 with destinations at nodes 10 and 12 within a day starting from 8 AM to 5:30 PM for medium demand case in the hypothetical dataset. We have assumed that 70% of the demand originates from node 1 and goes to node 10, and the rest moves towards node 12. The results indicate the essence of having charging facilities at nodes 5 and 7 with the capacity of 5 and 3 chargers to satisfy the medium demand (and reduce the number of lost users due to the range anxiety concern). Besides, Figure 5(b) shows the maximum distance traveled from the last visited charging facility. Figures 5(a) and 5(b) show that the charging facilities are selected in a way that EVs do not exceed the travel range of 200 miles in this network.

Figure 6 shows the distribution of charging prices for the selected facilities at nodes 5 and 7 with respect to EV users' arrivals over the planning horizon. Facility at node 5 offers a higher charging price compared to facility at node 7 due

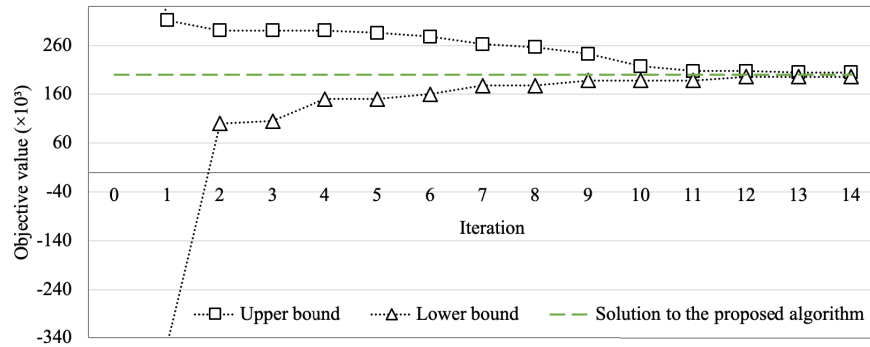


Fig. 9. Convergence of upper bound and lower bound (\$) for the solution of bi-level optimization model.

to higher demand from node 1 to node 10. As shown in Figure 6, charging prices are responsive to the EV arrivals. It can be observed that a high demand in the morning (e.g., 9 AM - 11 AM) and evening (e.g., 4 PM - 5:30 PM) causes a surge in charging prices as EV users have to wait to find a vacant charging spot. We also notice a decrease in prices in periods with less EV arrivals, where more chargers are available.

Figure 7 presents the average price of charging facilities within a day starting from 8 AM to 5:30 PM for the low, medium, and high demand levels in the hypothetical dataset. As indicated, charging prices vary with respect to the users' arrivals and facilities' occupancy. At the beginning of the planning horizon, prices are close to their minimum values since charging facilities are not fully occupied. As users from previous time steps as well as newly arrived users occupy the available spots, prices tend to increase.

As Figure 7 indicates, the average and standard deviation of charging prices increase by 4.5% and 13.5% in the medium demand case compared to the low demand case. The standard deviation captures the reaction of charging facility agencies to the number of EV users who search for vacant chargers over time. Moreover, the fluctuation of charging prices increases over the time steps with more EV arrivals, which shows the capability of the proposed approach to adjust the charging prices based on the observed demand. Figure 8 presents the number of required chargers for various demand distributions. As indicated, charging network operator shall install a charging facility at node 5 to serve EV users in all demand levels, although the number of chargers depend on the demand intensity. The same trend is observed regarding facility at node 7. However, facility at node 4 is installed only when high demand is experienced.

2) *Benchmark*: To theoretically evaluate the solution quality of the proposed algorithm, an alternative solution technique is implemented to solve the bi-level problem (4a)-(4i), (6a)-(6f), and (3) over the entire planning horizon. The system-level bi-level optimization method [55] generates theoretical lower and upper bounds to the proposed bi-level problem. To find the lower-bound, a system-level optimization problem is solved that includes the upper-level objective function (4a), constraints of both upper-level and lower-level problems (4b)-(4i) and (6b)-(6f), and parametric upper-bound of the optimal solution to the lower-level problem. The parametric upper-bound

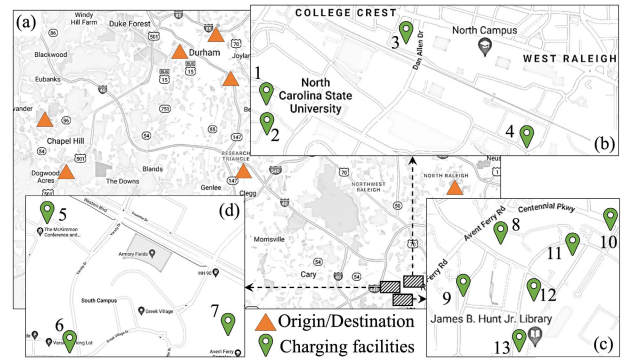


Fig. 10. (a) Travel origins/destinations, NC; (b),(c),(d) Charging facility locations on North Carolina State University campus. [Map source: Google, accessed November 25, 2020].

can be improved iteratively by adding new constraints to the system-level optimization problem through the following steps. First, the lower-level problem (6a)-(6f) is solved to system-level optimality given the value of upper-level decision variables (y, η, p, f) from the previous iteration. Then, admissible values of the lower-level decisions (x, z, v) , given the optimal objective value of lower-level problem (6a)-(6f), developed in the first step, are found. Finally, a tighter bound among all feasible-region bounds for upper-level decisions, i.e., (y, η, p, f) , is obtained that satisfies the constraints of the lower-level problem. To find the upper-bound, similar system-level optimization problem is solved under constraints of the lower-level problem (6a)-(6f), given the values of upper-level decision variables (y, η, p, f) found in the lower-bound procedure.

Figure 9 shows the convergence of upper and lower bounds with a gap of 4.5% for the bi-level optimization program, while the objective value obtained from the proposed methodology in Section IV is 200,160.5 (i.e., within a tight gap). The CPU time for the exact benchmark approach and the proposed algorithm is 173.1 hr and 2.3 hr, respectively, which indicates the computational efficiency of the proposed algorithm.

B. Real-World Dataset

The proposed formulation and solution technique are applied to a real-world case study in North Carolina. The network includes 42 nodes, 451 arcs, and 13 candidate locations for

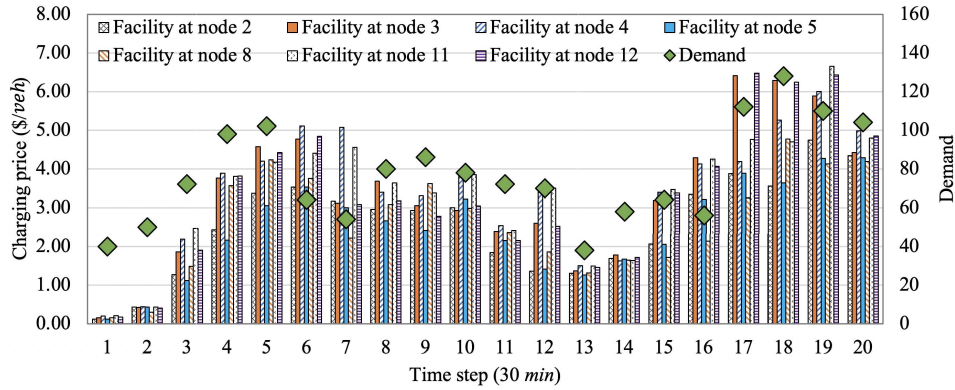


Fig. 11. Charging price at selected facilities over the planning horizon.

charging facility deployment, each with a 8-charger capacity, in North Carolina State University campus as shown in Figure 10. The figure indicates the origin and destination nodes of EV travellers (i.e., faculty, staff, students, and visitors) who tend to charge at a facility on campus for one time step. The origins and destinations are located in Raleigh, Durham, and Chapel Hill. We set $\alpha = 365$. The charging price is assumed to vary between a minimum of $l_i = 0.1(\$/veh)$ and maximum of $l'_i = 10.0(\$/veh)$, $\forall i \in N$, per time step. The pricing bounds can be estimated based on the amount of energy (e.g., in kilowatt hours) consumed in an EV multiplied by the car's driving range limit (e.g., in kilowatts per hour) for a variety of EVs and charger types given the electricity cost at different locations per time unit. The maximum driving range is assumed to be 200 miles. The medium demand in this dataset is distributed over time as 70, 105, 85, 60, and 115 vehicles for early AM, AM peak, mid-day, PM peak, and evening time-of-days. Similar to the hypothetical dataset, the low and high demand levels are assumed to be half and twice of the medium demand level, respectively. The initial SOC of EVs follow a normal distribution with an average of 50 miles and standard deviation of 20 miles.

Similar to the hypothetical dataset, Figure 11 indicates the average price of charging facilities with respect to EV arrivals within a day starting from 8 AM to 5:30 PM for the medium demand case. As illustrated, the proposed dynamic pricing policy increases the charging prices when the facilities are occupied by users from previous time steps and/or new EV arrivals. The prices decrease when the charging facilities offer available spots. Besides, Figure 11 presents the impact of charging facility locations on the pricing scheme. For example, facility at node 12 is located in the parking facility close to the main library. As expected, this charging facility experiences a high demand for EV charging throughout the day and hence, it offers the highest charging price in most time steps compared to other facilities. However, charging facility at node 3 (located near the student center building with generally less demand) is priced close to facility at node 2 and even higher in time step 17 due to excessive demand during the evening hours. An average demand of 87 users will be assigned to 13 facilities each with an 8-charger capacity (i.e., 104 charging spots) in 20 time steps that results in 7,539,121 decision variables. The proposed iterative active-set algorithm completes within

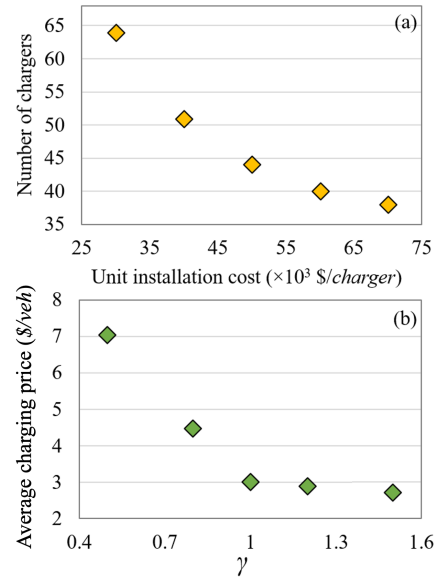


Fig. 12. Sensitivity of upper-level objective function terms to model parameters: (a) number of chargers versus unit installation cost and (b) average charging price versus coefficient of charging price term in the lower-level problem (i.e., cost-to-monetary value conversion factor γ).

263 iterations, with a 0.43% gap, for the given travel times in MSA.

C. Sensitivity Analyses

Besides Figure 8 on the sensitivity of selected chargers given various demand distributions, we have conducted a series of sensitivity analysis on various parameter values, i.e., C_i and γ , to evaluate the impact of charging facility installation cost and pricing scheme on the objective value (captured by (11)), as illustrated in Figure 12. When the value of unit installation cost at each station, i.e., C_i , increases, so does the objective value term on the installation cost (see Figure 12 (a)), which indicates a negative impact on adding more chargers due to the increase in total cost. According to Figure 12 (b), when the value of γ increases, the average charging prices decrease to improve the utilization by reducing the number of lost users affected by the pricing scheme at charging facilities. The inverse relationship between γ and charging price can be interpreted by the monotonic nature of the travel time function

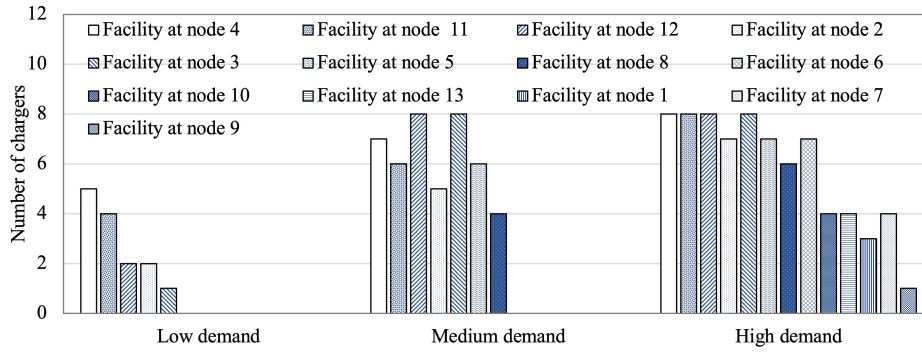


Fig. 13. Charging network design for the low, medium, and high demand cases in real-world dataset.

TABLE II
SENSITIVITY OF CHARGING PRICE TO THE NUMBER OF CHARGERS

Max # chargers (η_{max})	Avg charging price (\$/veh) per time step	Avg price std
8	3.03	0.56
15	2.95	0.82
20	2.73	1.04

as well. The value of γ balances the impact of travel costs versus charging prices, as indicated in (10).

Additionally, Figure 13 shows the optimal network design and capacity of charging facilities at different demand levels. As expected, higher demand requires higher number of chargers. If the capacity of existing facilities is reached, additional facilities will be needed to satisfy the demand (e.g., Facility at nodes 1, 6, 7, 9, 10, and 13 under high demand). Furthermore, Table II shows the impact of maximum number of chargers η_{max} on average charging price and its standard deviation. As indicated, when η_{max} increases, the charging prices decrease on average due to the availability of additional supply. Besides, it can motivate EV users to move towards the central locations of the campus for charging, where the destinations $d \in D$ are located. Therefore, popular charging facilities (e.g., closer to the main library) will keep their high charging prices due to excessive arrivals. On the other hand, charging facilities that are far from the campus center will reduce their prices to offer more incentives to EV users. The observed pricing scheme affects the EV user decisions and as a result, facility selection behaviors will be more diverse. This impact is shown in Table II by the increasing trend in the standard deviations. Higher utilization rate in popular charging facilities causes distant facilities to reduce their prices more to stay competitive. This increases the deviations of charging prices among different facilities.

Figure 14 presents the average number of charging attempts versus maximum driving range limits (offered by different manufacturers) at medium and high demand levels in the hypothetical case study. Moreover, Figure 14 indicates that the number of charging attempts changes inversely with the maximum driving range changes. Note that, lower driving range limits impose higher facility deployment costs due to the need for more frequent charging visits and consequently, higher number of facilities. For instance, driving range of

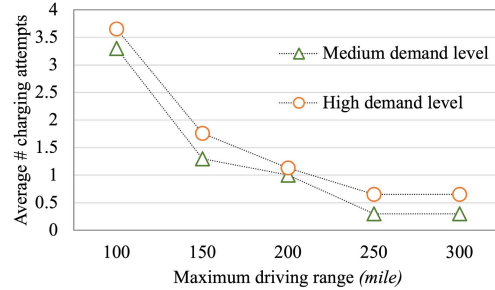


Fig. 14. Sensitivity to maximum driving range in medium and high demand levels in hypothetical case study.

TABLE III
SENSITIVITY OF THE NUMBER OF SELECTED FACILITIES TO DIFFERENT RANGE LIMITS IN HYPOTHETICAL CASE STUDY

Max range limit	Selected nodes to install facility	
	Medium demand	High demand
100	2,3,4,5,7,8,9	2,3,4,5,7,8,9
150	3,4,9	3,4,6,8,9
200	5,7	4,5,7
250	7	5,7
300	7	5,7

100 miles enforces the charging network operator to install charging facilities at nodes 2,3,4,5,7,8, and 9 in the high demand level, while driving range of 300 miles requires facility deployments at nodes 5 and 7. Similarly, Table III presents the nodes that are selected for charging facility deployment based on the maximum driving range in medium and high demand levels. The decreasing trend in the number of charging facilities with the increase in the driving range limit is observed in more details.

VI. CONCLUSION

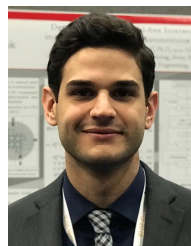
This paper develops a methodology that incorporates a dynamic pricing scheme into EV charging infrastructure design. The objective is to determine the optimal (i) number, location, and capacity of charging facilities in the transportation network and (ii) demand-driven charging pricing scheme. The problem is formulated as a bi-level mathematical program that includes the EV charging facility design and pricing scheme in the upper level and user charging decisions with respect to charging pricing and travel time in the lower level. The model minimizes the total costs including infrastructure investments and operating costs of facilities as

well as users' travel and charging expenses under equilibrium flows. The bi-level problem is converted into an equivalent single-level formulation following the redefinition of binary decision variables as continuous variables, and solved using an active-set based methodology where arc travel times are estimated using an MFD-based technique. MFD generates the travel time function based on the arc flow, which is updated based on the active-set solutions in each iteration. Additionally, a stochastic queuing theory is utilized to establish a linear relationship between each facility's occupancy and physical capacity to capture the impact of waiting time on maximum occupancy. Numerical experiments include (i) a hypothetical network and (ii) a real-world case study in North Carolina. The numerical results indicate that the proposed algorithm can solve the problem effectively. Besides, the solution to the proposed algorithm falls within a tight theoretical gap (obtained from an exact solution technique applied to the original bi-level problem), which indicates the solution quality and computational efficiency (i.e., the CPU time of 2.3 *hr* compared to 173.1 *hr* of the exact algorithm on a hypothetical dataset) of the proposed methodology. A series of sensitivity analyses has been conducted to study the impact of input parameters on the solutions and draw managerial insights. Future research can be conducted in a few directions. It is very interesting to include a multi-agency competitions to absorb EV users to respective charging facilities in highly-variable demand regions. Furthermore, the impact of various EV penetration rates can be incorporated in the study to obtain more realistic resolutions for the existing traffic conditions. The impact of charging decisions on traffic system dynamics, also considering automated traffic streams [56], [57], [58], [59], [60], [61], as well as traffic control decisions [62], [63] on drivers' charging attempts are other interesting directions. Besides, it will be very encouraging to study the electrification of heavy equipment and its impact on charging location design and management strategies, e.g., using approaches used for service truck logistics [64], emergency response planning [65], micromobility logistics, among others. It will be worthwhile to incorporate the charging demand uncertainties (e.g., due to special events and holidays) into the proposed pricing framework over long-term study periods. Another direction will be to study stochastic latency along network routes with various traveling behaviors and uncertain travel times compared to the Wardrop equilibrium [66].

REFERENCES

- [1] BTS. (2020). *Hybrid-Electric, PLUG-in Hybrid-Electric and Electric Vehicle Sales*. Bureau of Transportation Statistics. Accessed: May 13, 2020. [Online]. Available: <https://www.bts.gov/content/gasoline-hybrid-and-electric-vehicle-sales>
- [2] F. Xie, C. Liu, S. Li, Z. Lin, and Y. Huang, "Long-term strategic planning of inter-city fast charging infrastructure for battery electric vehicles," *Transp. Res. E, Logistics Transp. Rev.*, vol. 109, pp. 261–276, Jan. 2018.
- [3] M. Ghamami, Y. Nie, and A. Zockaie, "Planning charging infrastructure for plug-in electric vehicles in city centers," *Int. J. Sustain. Transp.*, vol. 10, no. 4, pp. 343–353, 2016.
- [4] H. Zheng and S. Peeta, "Routing and charging locations for electric vehicles for intercity trips," *Transp. Planning Technol.*, vol. 40, no. 4, pp. 393–419, May 2017.
- [5] Y. Li, P. Zhang, and Y. Wu, "Public recharging infrastructure location strategy for promoting electric vehicles: A bi-level programming approach," *J. Clean. Prod.*, vol. 172, pp. 2720–2734, Jan. 2018.
- [6] M. J. Hodgson, "A flow-capturing location-allocation model," *Geogr. Anal.*, vol. 22, no. 3, pp. 270–279, Jul. 1990.
- [7] O. Berman, D. Krass, and C. W. Xu, "Locating flow-intercepting facilities: New approaches and results," *Ann. Oper. Res.*, vol. 60, no. 1, pp. 121–143, Dec. 1995.
- [8] M. J. Hodgson, "A billboard location model," *Geographical Environ. Model.*, vol. 1, pp. 25–45, Jan. 1997.
- [9] A. Shukla, J. Pekny, and V. Venkatasubramanian, "An optimization framework for cost effective design of refueling station infrastructure for alternative fuel vehicles," *Comput. Chem. Eng.*, vol. 35, no. 8, pp. 1431–1438, Aug. 2011.
- [10] O. Arslan and O. E. Karaşan, "A benders decomposition approach for the charging station location problem with plug-in hybrid electric vehicles," *Transp. Res. B, Methodol.*, vol. 93, pp. 670–695, Nov. 2016.
- [11] C. Lee and J. Han, "Benders-and-price approach for electric vehicle charging station location problem under probabilistic travel range," *Transp. Res. B, Methodol.*, vol. 106, pp. 130–152, Dec. 2017.
- [12] X. Li, J. Ma, J. Cui, A. Ghiasi, and F. Zhou, "Design framework of large-scale one-way electric vehicle sharing systems: A continuum approximation model," *Transp. Res. B, Methodol.*, vol. 88, pp. 21–45, Jun. 2016.
- [13] S. Faridimehr, S. Venkatachalam, and R. B. Chinnam, "A stochastic programming approach for electric vehicle charging network design," 2017, *arXiv:1701.06723*.
- [14] Y. Hua, D. Zhao, X. Wang, and X. Li, "Joint infrastructure planning and fleet management for one-way electric car sharing under time-varying uncertain demand," *Transp. Res. B, Methodol.*, vol. 128, pp. 185–206, Oct. 2019.
- [15] L. Hajibabai, A. Atik, and A. Mirheli, "Joint power distribution and charging network design for electrified mobility with user equilibrium decisions," *Comput.-Aided Civil Infrastruct. Eng.*, vol. 38, no. 3, pp. 307–324, 2023, doi: [10.1111/micc.12854](https://doi.org/10.1111/micc.12854).
- [16] A. Mirheli and L. Hajibabai, "Hierarchical optimization of charging infrastructure design and facility utilization," *IEEE Trans. Intell. Transp. Syst.*, vol. 23, no. 9, pp. 15574–15587, Sep. 2022, doi: [10.1109/TITS.2022.3142196](https://doi.org/10.1109/TITS.2022.3142196).
- [17] A. Mirheli and L. Hajibabai, "Charging infrastructure and pricing strategy: How to accommodate different perspectives?" in *Proc. IEEE 23rd Int. Conf. Intell. Transp. Syst. (ITSC)*, Sep. 2020, pp. 1–5.
- [18] E. Bardaka, L. Hajibabai, and M. P. Singh, "Reimagining ride sharing: Efficient, equitable, sustainable public microtransit," *IEEE Internet Comput.*, vol. 24, no. 5, pp. 38–44, Sep. 2020.
- [19] H. Zheng, X. He, Y. Li, and S. Peeta, "Traffic equilibrium and charging facility locations for electric vehicles," *Netw. Spatial Econ.*, vol. 17, no. 2, pp. 435–457, Jun. 2017.
- [20] F. He, D. Wu, Y. Yin, and Y. Guan, "Optimal deployment of public charging stations for plug-in hybrid electric vehicles," *Transp. Res. B, Methodol.*, vol. 47, pp. 87–101, Jan. 2013.
- [21] C. Q. Tran, D. Ngoduy, M. Keyvan-Ekbatani, and D. Watling, "A user equilibrium-based fast-charging location model considering heterogeneous vehicles in urban networks," *Transportmetrica A, Transp. Sci.*, vol. 17, no. 4, pp. 439–461, Dec. 2021.
- [22] X. Zhang, D. Rey, and S. T. Waller, "Multitype recharge facility location for electric vehicles," *Comput.-Aided Civil Infrastruct. Eng.*, vol. 33, no. 11, pp. 943–965, Nov. 2018.
- [23] F. He, Y. Yin, and J. Zhou, "Deploying public charging stations for electric vehicles on urban road networks," *Transp. Res. C, Emerg. Technol.*, vol. 60, pp. 227–240, Nov. 2015.
- [24] J. He, H. Yang, T.-Q. Tang, and H.-J. Huang, "An optimal charging station location model with the consideration of electric vehicle's driving range," *Transp. Res. C, Emerg. Technol.*, vol. 86, pp. 641–654, Jan. 2018.
- [25] Z. Chen, W. Liu, and Y. Yin, "Deployment of stationary and dynamic charging infrastructure for electric vehicles along traffic corridors," *Transp. Res. C, Emerg. Technol.*, vol. 77, pp. 185–206, Apr. 2017.
- [26] R. Riemann, D. Z. W. Wang, and F. Busch, "Optimal location of wireless charging facilities for electric vehicles: Flow-capturing location model with stochastic user equilibrium," *Transp. Res. C, Emerg. Technol.*, vol. 58, pp. 1–12, Sep. 2015.
- [27] W. Jing, K. An, M. Ramezani, and I. Kim, "Location design of electric vehicle charging facilities: A path-distance constrained stochastic user equilibrium approach," *J. Adv. Transp.*, vol. 2017, pp. 1–15, Oct. 2017.
- [28] C. Lei, L. Lu, and Y. Ouyang, "System of systems model for planning electric vehicle charging infrastructure in intercity transportation networks under emission consideration," *IEEE Trans. Intell. Transp. Syst.*, vol. 23, no. 7, pp. 8103–8113, Jul. 2022.

- [29] X. Chen, Z. Li, H. Dong, Z. Hu, and C. C. Mi, "Enabling extreme fast charging technology for electric vehicles," *IEEE Trans. Intell. Transp. Syst.*, vol. 22, no. 1, pp. 466–470, Jan. 2021.
- [30] H. Ko, S. Pack, and V. C. M. Leung, "An optimal battery charging algorithm in electric vehicle-assisted battery swapping environments," *IEEE Trans. Intell. Transp. Syst.*, vol. 23, no. 5, pp. 3985–3994, May 2022.
- [31] J. He, N. Yan, J. Zhang, Y. Yu, and T. Wang, "Battery electric buses charging schedule optimization considering time-of-use electricity price," *J. Intell. Connected Vehicles*, vol. 5, no. 2, pp. 138–145, May 2022.
- [32] G. Guo and T. Xu, "Vehicle rebalancing with charging scheduling in one-way car-sharing systems," *IEEE Trans. Intell. Transp. Syst.*, vol. 23, no. 5, pp. 4342–4351, May 2020.
- [33] Y. Wang, J. Bi, W. Guan, C. Lu, and D. Xie, "Optimal charging strategy for intercity travels of battery electric vehicles," *Transp. Res. D, Transp. Environ.*, vol. 96, Jul. 2021, Art. no. 102870.
- [34] O. N. Nezamuddin, C. L. Nicholas, and E. C. D. Santos, "The problem of electric vehicle charging: State-of-the-art and an innovative solution," *IEEE Trans. Intell. Transp. Syst.*, vol. 23, no. 5, pp. 4663–4673, May 2022.
- [35] L. Zhang, Z. Zeng, and K. Gao, "A bi-level optimization framework for charging station design problem considering heterogeneous charging modes," *J. Intell. Connected Vehicles*, vol. 5, no. 1, pp. 8–16, Feb. 2022.
- [36] Y. Wang, J. Bi, W. Guan, and X. Zhao, "Optimising route choices for the travelling and charging of battery electric vehicles by considering multiple objectives," *Transp. Res. D, Transp. Environ.*, vol. 64, pp. 246–261, Oct. 2018.
- [37] Y. Liu, L. Wang, Z. Zeng, and Y. Bie, "Optimal charging plan for electric bus considering time-of-day electricity tariff," *J. Intell. Connected Vehicles*, vol. 5, no. 2, pp. 123–137, May 2022.
- [38] D. Mackowski, Y. Bai, and Y. Ouyang, "Parking space management via dynamic performance-based pricing," *Transp. Res. C, Emerg. Technol.*, vol. 59, pp. 66–91, Oct. 2015.
- [39] A. Mirheli and L. Hajibabai, "Utilization management and pricing of parking facilities under uncertain demand and user decisions," *IEEE Trans. Intell. Transp. Syst.*, vol. 21, no. 5, pp. 2167–2179, May 2020.
- [40] R. H. Pratt, "Introduction," in *Traveler Response to Transportation System Changes Handbook*, 3rd ed. Washington, DC, USA: National Academies, 2013, ch. 1, pp. 42–66.
- [41] Y. Sheffi, *Urban Transportation Networks*. Cambridge, MA, USA: Massachusetts Institute of Technology, 1985.
- [42] L. Zhang, S. Lawphongpanich, and Y. Yin, "An active-set algorithm for discrete network design problems," in *Transportation and Traffic Theory 2009: Golden Jubilee*. Cham, Switzerland: Springer, 2009, pp. 283–300.
- [43] D. Bertsimas and J. N. Tsitsiklis, *Introduction to Linear Optimization*, vol. 6. Belmont, MA, USA: Athena Scientific, 1997.
- [44] L. Hajibabai, Y. Bai, and Y. Ouyang, "Joint optimization of freight facility location and pavement infrastructure rehabilitation under network traffic equilibrium," *Transp. Res. B, Methodol.*, vol. 63, pp. 38–52, May 2014.
- [45] H. Farvaresh and M. M. Sepehri, "A single-level mixed integer linear formulation for a bi-level discrete network design problem," *Transp. Res. E, Logistics Transp. Rev.*, vol. 47, no. 5, pp. 623–640, Sep. 2011.
- [46] F. Facchinei and J.-S. Pang, *Finite-Dimensional Variational Inequalities and Complementarity Problems*. Cham, Switzerland: Springer, 2007.
- [47] (2018). *IBM ILOG CPLEX Optimization Studio CPLEX User Manual*. [Online]. Available: <https://www.ibm.com/analytics/cplex-optimizer>
- [48] A. Hajbabaie and R. F. Benekohal, "A program for simultaneous network signal timing optimization and traffic assignment," *IEEE Trans. Intell. Transp. Syst.*, vol. 16, no. 5, pp. 2573–2586, Oct. 2015.
- [49] *U.S. Bureau of Public Roads. Urban Transportation Planning*, BPR, General Information and Introduction to System, U.S. Department of Transportation, Washington, DC, USA, 1970.
- [50] M. Yildirimoglu and N. Geroliminis, "Approximating dynamic equilibrium conditions with macroscopic fundamental diagrams," *Transp. Res. B, Methodol.*, vol. 70, pp. 186–200, Dec. 2014.
- [51] M. Yildirimoglu, M. Ramezani, and N. Geroliminis, "Equilibrium analysis and route guidance in large-scale networks with MFD dynamics," *Transp. Res. Proc.*, vol. 9, pp. 185–204, Jan. 2015.
- [52] W. B. Powell and Y. Sheffi, "The convergence of equilibrium algorithms with predetermined step sizes," *Transp. Sci.*, vol. 16, no. 1, pp. 45–55, Feb. 1982.
- [53] R. Mounce and M. Carey, "On the convergence of the method of successive averages for calculating equilibrium in traffic networks," *Transp. Sci.*, vol. 49, no. 3, pp. 535–542, Aug. 2015.
- [54] Y. Lin and L. Schrage, "The global solver in the LINDO API," *Optim. Methods Softw.*, vol. 24, nos. 4–5, pp. 657–668, Aug. 2009.
- [55] A. Mitsos, P. Lemonidis, and P. I. Barton, "Global solution of bilevel programs with a nonconvex inner program," *J. Global Optim.*, vol. 42, no. 4, pp. 475–513, Dec. 2008.
- [56] R. Niroumand, L. Hajibabai, and A. Hajbabaie, "White phase intersection control through distributed coordination: A prosocial mobile controller paradigm in a mixed traffic stream," *IEEE Trans. Intell. Transp. Syst.*, to be published.
- [57] X. Li, "Trade-off between safety, mobility and stability in automated vehicle following control: An analytical method," *Transp. Res. B, Methodol.*, vol. 166, pp. 1–18, Dec. 2022.
- [58] R. Niroumand, M. Tajalli, L. Hajibabai, and A. Hajbabaie, "Joint optimization of vehicle-group trajectory and signal timing: Introducing the white phase for mixed-autonomy traffic stream," *Transp. Res. C, Emerg. Technol.*, vol. 116, Jul. 2020, Art. no. 102659.
- [59] R. Niroumand, M. Tajalli, L. Hajibabai, and A. Hajbabaie, "The effects of the 'white phase' on intersection performance with mixed-autonomy traffic stream," in *Proc. IEEE 23rd Int. Conf. Intell. Transp. Syst. (ITSC)*, Sep. 2020, pp. 1–6.
- [60] A. Mirheli, M. Tajalli, L. Hajibabai, and A. Hajbabaie, "A consensus-based distributed trajectory control in a signal-free intersection," *Transp. Res. C, Emerg. Technol.*, vol. 100, pp. 161–176, Mar. 2019.
- [61] A. Mirheli, L. Hajibabai, and A. Hajbabaie, "Development of a signal-head-free intersection control logic in a fully connected and autonomous vehicle environment," *Transp. Res. C, Emerg. Technol.*, vol. 92, pp. 412–425, Jul. 2018.
- [62] A. Hajbabaie, J. C. Medina, and R. F. Benekohal, "Effects of its-based left turn policies on network performance," in *Proc. 13th Int. IEEE Conf. Intell. Transp. Syst.*, Sep. 2010, pp. 80–84.
- [63] J. C. Medina, A. Hajbabaie, and R. F. Benekohal, "Arterial traffic control using reinforcement learning agents and information from adjacent intersections in the state and reward structure," in *Proc. 13th Int. IEEE Conf. Intell. Transp. Syst.*, Sep. 2010, pp. 525–530.
- [64] L. Hajibabai and Y. Ouyang, "Planning of resource replenishment location for service trucks under network congestion and routing constraints," *Transp. Res. Rec. J. Transp. Res. Board*, vol. 2567, pp. 10–17, Jan. 2016.
- [65] A. Atik and L. Hajibabai, "Location and allocation of incident respondents under severity levels and capacity constraints: Formulation, methodology, and application," in *Proc. IEEE Int. Intell. Transp. Syst. Conf. (ITSC)*, Sep. 2021, pp. 2181–2186.
- [66] A. Yekkehkhany and R. Nagi, "Risk-averse equilibria for vehicle navigation in stochastic congestion games," *IEEE Trans. Intell. Transp. Syst.*, vol. 23, no. 10, pp. 18719–18735, Oct. 2022.



Amir Mirheli received the B.Sc. degree from the Sharif University of Technology in 2013 and the M.Sc. degree from the University of Tehran in 2015. He is currently pursuing the Ph.D. degree in operations research with North Carolina State University (NCSU). His research interests include systems analytics and optimization for transportation systems and logistics with uncertainties.



Leila Hajibabai (Member, IEEE) received the Ph.D. degree from the University of Illinois at Urbana–Champaign in 2014 and the dual M.Sc. degree from the University of Tehran and UIUC. She is currently an Assistant Professor with the Department of Industrial and Systems Engineering, NCSU. Her research interests include supply chain logistics and systems analytics and optimization. She is also a member of INFORMS and TRB. She is also the Chair of TRB's Joint Young Members Subcommittee of Highway Maintenance and Operations Sections.